Journal of Structural Engineering & Applied Mechanics (2025) 8(4):362-372
DOI 10.31462/jseam.2025.04362372

RESEARCH ARTICLE

Contact problem of a functionally graded isotropic layer supported by a Kerr foundation

Ilkem Turhan Cetinkaya[1], Pembe Merve Karabulut[2], Huseyin Oguz[1], Isa Comez[3*]

[1] Kütahya Dumlupınar University, Department of Mathematics, Science and Art Faculty, Kütahya, Türkiye
[2] Çankırı Karatekin University, Civil Engineering Department, Çankırı, Türkiye
[3] Karadeniz Technical University, Department of Civil Engineering, Engineering Faculty, Trabzon, Türkiye

Article History

Received 06 November 2025
Accepted 25 December 2025

Keywords

Contact mechanics
Kerr foundation
Functionally graded materials
Fourier transform
Singular integral equation

Abstract

In this study, the contact problem in a functionally graded (FG) layer resting on a Kerr foundation is considered. The Kerr foundation is a foundation system that has two springs with a shear plate in between. It is assumed that the thickness of the FG isotropic layer is h, and it is indented by a cylindrical punch. Moreover, the layer is loaded by a concentrated force. The shear modulus of the layer is assumed to vary exponentially in the thickness direction. The body forces are neglected. The boundary conditions of the problem are determined considering the geometry of the problem. The problem is modeled as a singular integral equation using the Fourier integral transform technique, the basic equations of elasticity theory, and the boundary conditions of the problem. The singular integral equation is solved numerically using the Gauss-Chebyshev method, in which the singular integral equation leads to a system of algebraic equations. The effects of material inhomogeneity, indentation load, and foundation parameters on the contact behavior are examined. The detailed mechanical analysis is presented.

1. Introduction

Contact problems are crucial subjects in mechanics. Since the bodies are in contact with each other, stress and deformations occur in the contact regions. The analytical and numerical studies are improved to examine the behavior of the contact. Among the various numerical techniques, the Gauss-Chebyshev method is a particularly effective method for solving the singular integral equations arising in contact problems. The Gauss-Chebyshev method is applied to a two-dimensional Hertzian contact problem with surface tension by Long et al. [1]. Yusufoğlu and Turhan [2, 3] consider a strip problem under plane strain conditions. While the problem is solved by an iterative method in [2], the same problem is solved by the Gauss-Chebyshev method in [3]. Çakıroğlu et al. [4] consider the continuous and discontinuous contact problem of two elastic layers resting on an elastic semi-infinite plane. Stress distributions are determined with the help of Gauss-Chebyshev integration formulas. Yan and Mi [5] solve a receding contact problem semi-analytically. More studies in which the Gauss-Chebyshev method is applied to the singular integral equations arising from contact problems can be seen in the references [6-10].

* Corresponding author (isacomez@ktu.edu.tr)
eISSN 2630-5763

Material properties are important in mechanical problems. One of the common materials is functionally graded materials (FGMs). FGMs are inhomogeneous composites whose material properties vary continuously along one or more spatial directions. Mechanical problems in the functionally graded (FG) layers have been widely studied recently. Çömez [11] presents a detailed analysis of a cylindrical punch problem in an FG layer. Karabulut et al. [12] consider an FG orthotropic coated half-plane problem caused by a moving punch. El-Borgi et al. [13] studied a frictionless receding contact between an elastic functionally graded layer and a homogeneous half-space. Öner [14] presents a frictionless contact problem in an FGM coating and orthotropic substrate. Numerical results for three different orthotropic materials are presented. One can check some other studies indicating the contact problems of FGM in [15-20].

Kerr-type foundations developed by Kerr [21] play an important role in contact mechanics. In Kerr-type foundation models, the interaction between the structure and the supporting medium can be modeled more realistically than in the Winkler or Pasternak foundations. Some of the studies in Kerr-type foundations can be summarized as follows:

Zhang et al. [22] proposed a Kerr-type elastic foundation model of a beam bonded on an elastic layer. The Finite Element method is applied. Timesli [23] developed an explicit analytical model for the buckling of a porous FGM cylindrical shell. Shahsavari et al. [24] developed a Galerkin method for the eigenvalue problem of the quasi-3D hyperbolic plate model of FG plates resting on Winkler, Pasternak, and Kerr foundations. Paliwal and Ghosh [25] presented the stability of orthotropic plates on a Kerr Foundation. Comparison of nondimensional critical loads for a plate resting on Winkler, Pasternak, and Kerr foundations is presented. Besides, some studies about the Kerr foundation are also published in [26-30].

Although the contact problems of a Winkler-Pasternak foundation have been studied by many researchers, the contact problems of a Kerr foundation have not been investigated yet. To fill this gap in the literature, the present study considers the contact problem between the rigid cylindrical punch and an FG isotropic layer on a Kerr foundation. The frictionless plane strain contact problem is solved by applying elasticity theory and the Fourier transform.

2. Formulation of the problem

This section presents the formulation of the symmetric plane strain contact problem given in Fig. 1. The layer is an FG elastic layer, and the layer of thickness h is assumed to be supported by an elastic foundation of Kerr type. A Kerr-type foundation is a foundation system that has two springs with a shear plate in between. The layer is loaded by a concentrated force P through a rigid cylindrical punch with radius R. In this problem, the effect of body forces is neglected.

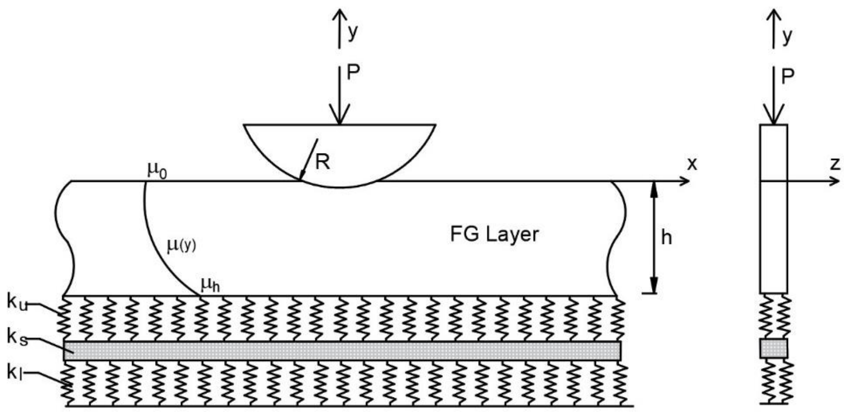

Fig. 1. Geometry of the FG isotropic layer indented by a cylindrical punch

The shear modulus μ is assumed to vary exponentially through the thickness of the layer as

$$\mu(y) = \mu_0 e^{\gamma y} \tag{1}$$

where μ_0 is the shear modulus on the top surface of the layer, and γ is a constant characterizing the material inhomogeneity.

Hook's law can be written under the assumption that the FG layer is isotropic at every point, as follows

$$\sigma_x(x,y) = \frac{\mu(y)}{\kappa-1}\left[(\kappa+1)\frac{\partial u}{\partial x} + (3-\kappa)\frac{\partial v}{\partial y}\right] \tag{2a}$$

$$\sigma_y(x,y) = \frac{\mu(y)}{\kappa-1}\left[(3-\kappa)\frac{\partial u}{\partial x} + (\kappa+1)\frac{\partial v}{\partial y}\right] \tag{2b}$$

$$\tau_{xy} = \mu(y)\left[\frac{\partial u}{\partial y} + \frac{\partial v}{\partial x}\right] \tag{2c}$$

where u,v are the components of the displacement vectors on the axis $x-$ and $y-$, respectively. Moreover, $\kappa = 3-4\nu$ for the plane strain, where ν is Poisson's ratio that is taken as a constant.

Substituting Hooke's law defined by Eqs. (2) into the equilibrium equations, the following system of partial differential equations, where the unknowns are the displacements $u(x,y)$ and $v(x,y)$, are obtained as

$$(\kappa+1)\frac{\partial^2 u}{\partial x^2} + (\kappa-1)\frac{\partial^2 u}{\partial y^2} + 2\frac{\partial^2 v}{\partial x \partial y} + \gamma(\kappa-1)\left[\frac{\partial u}{\partial y} + \frac{\partial v}{\partial x}\right] = 0 \tag{3a}$$

$$(\kappa-1)\frac{\partial^2 v}{\partial x^2} + (\kappa+1)\frac{\partial^2 v}{\partial y^2} + 2\frac{\partial^2 u}{\partial x \partial y} + \gamma\left[(3-\kappa)\frac{\partial u}{\partial x} + (\kappa+1)\frac{\partial v}{\partial y}\right] = 0 \tag{3b}$$

Considering the symmetry of the problem, the Fourier sine and cosine transforms of the displacements may be written.

$$u(x,y) = \frac{2}{\pi}\int_0^\infty \varphi(\alpha,y)\, sin(\alpha x) d\alpha \tag{4a}$$

$$v(x,y) = \frac{2}{\pi}\int_0^\infty \psi(\alpha,y)\, cos(\alpha x) d\alpha \tag{4b}$$

where $\varphi(\alpha,y)$ and $\psi(\alpha,y)$ are inverse Fourier transforms of $u(x,y)$ and $v(x,y)$, respectively. Substituting Eqs. (4) into Eqs. (3), and considering the inverse Fourier transforms, the following ordinary differential equations are obtained

$$-(\kappa+1)\alpha^2\varphi + (\kappa-1)\frac{d^2\varphi}{dy^2} - 2\alpha\frac{d\psi}{dy} + \gamma(\kappa-1)\left[\frac{d\varphi}{dy} - \alpha\psi\right] = 0 \tag{5a}$$

$$-(\kappa-1)\alpha^2\psi + (\kappa+1)\frac{d^2\psi}{dy^2} + 2\alpha\frac{d\varphi}{dy} + \gamma\left[(3-\kappa)\alpha\varphi + (\kappa+1)\frac{d\psi}{dy}\right] = 0 \tag{5b}$$

Let us seek the solution of the system of ordinary differential equations defined by Eqs. (5) as:

$$\varphi(y) = \sum_{j=1}^{4} A_j\, e^{n_j y} \tag{6a}$$

$$\psi(y)=\sum_{j=1}^{4}A_j\,m_j e^{n_j y} \tag{6b}$$

where A_j are the unknown functions that will be determined from the boundary conditions of the problem. The roots of the characteristic equation given by

$$n_j^4+2\gamma n_j^3+(\gamma^2-2\alpha^2)n_j^2-2\alpha^2\gamma n_j+\alpha^2(\alpha^2+\gamma^2\frac{3-\kappa}{1+\kappa})=0 \tag{7}$$

can be determined as follows:

$$n_1=-\frac{1}{2}\left(\gamma+\sqrt{4\alpha^2+\gamma^2+4i\alpha|\gamma|\sqrt{\frac{3-\kappa}{\kappa+1}}}\right) \tag{8a}$$

$$n_2=-\frac{1}{2}\left(\gamma+\sqrt{4\alpha^2+\gamma^2-4i\alpha|\gamma|\sqrt{\frac{3-\kappa}{\kappa+1}}}\right) \tag{8b}$$

$$n_3=-\frac{1}{2}\left(\gamma-\sqrt{4\alpha^2+\gamma^2+4i\alpha|\gamma|\sqrt{\frac{3-\kappa}{\kappa+1}}}\right) \tag{8c}$$

$$n_4=-\frac{1}{2}\left(\gamma-\sqrt{4\alpha^2+\gamma^2-4i\alpha|\gamma|\sqrt{\frac{3-\kappa}{\kappa+1}}}\right) \tag{8d}$$

and

$$m_j=\frac{(n_j+2\gamma\nu)\left(-2n_j^2(1-\nu)+2n_j\gamma(1-\nu)-\alpha^2(3-2\nu)\right)}{\alpha(\alpha^2-4\gamma^2(-1+\nu)\nu)} \tag{9}$$

Substituting Eqs. (4)-(6) into Eqs. (2), stress components for the layer are readily obtained as

$$\frac{\sigma_x(x,y)}{\mu_0}=\frac{2}{\pi}\int_0^\infty\sum_{j=1}^{4}\frac{A_j}{\kappa-1}\left[(3-\kappa)m_j n_j+\alpha(\kappa+1)\right]e^{(n_j+\gamma)y}\,cos(\,\alpha x)d\alpha \tag{10a}$$

$$\frac{\sigma_y(x,y)}{\mu_0}=\frac{2}{\pi}\int_0^\infty\sum_{j=1}^{4}\frac{A_j}{\kappa-1}\left[(\kappa+1)m_j n_j+\alpha(3-\kappa)\right]e^{(n_j+\gamma)y}\,cos(\,\alpha x)d\alpha \tag{10b}$$

$$\frac{\tau_{xy}(x,y)}{\mu_0}=\frac{2}{\pi}\int_0^\infty\sum_{j=1}^{4}A_j\left[(n_j-\alpha m_j)\right]e^{(n_j+\gamma)y}\,sin(\,\alpha x)d\alpha \tag{10c}$$

3. The boundary conditions and the singular integral equation

Boundary conditions of the contact problem include

$$\sigma_y(x,0) = \begin{Bmatrix} -p(x) & 0 \le x < a \\ 0 & a \le x < \infty \end{Bmatrix} \tag{11a}$$

$$\tau_{xy}(x,0) = 0 \qquad 0 \le x < \infty \tag{11b}$$

$$\tau_{xy}(x,-h) = 0 \quad 0 \le x < \infty \tag{11c}$$

$$\sigma_z(x,-h) = \frac{k_l k_u}{k_l + k_u} v(x,-h) - \frac{k_s k_u}{k_l + k_u} \frac{\partial^2 v(x,-h)}{\partial x^2} \qquad 0 \le x < \infty \tag{11d}$$

$$\frac{\partial v(x,0)}{\partial x} = F(x) \quad 0 \le x < \infty \tag{12}$$

where $p(x)$ is the unknown contact stress between the rigid punch and the layer on the contact area $(-a,a)$. The Kerr model foundation is a three-parameter elastic model that consists of an upper layer k_u, a shear layer$k_s$and a lower layer k_l. k_u, $k_s$and k_l represents the stiffness of the upper layer, the stiffness of the shear layer, and the stiffness of the lower layer, respectively. *F(x)* is the derivative of the profile of the rigid punch; one may write

$$F(x) = \frac{x}{R} \tag{13}$$

Applying the boundary conditions given by Eq. (11), four of the unknown functions A_j $(j = 1, \ldots, 4)$, appearing in the stress and the displacement expressions for the layer, may be eliminated in terms of the unknown contact stress $p(x)$. Substituting them into the rested boundary condition Eq. (12) and using the symmetry consideration, $p(x) = p(-x)$, the following Cauchy-type singular integral equation is obtained.

$$\frac{1}{\pi} \int_{-a}^{a} p(t) \left[\frac{1}{t-x} + k(x,t) \right] dt = \frac{\mu_0}{\beta} \frac{x}{R} \tag{14}$$

where

$$k(x,t) = \frac{1}{\beta} \int_0^\infty [M(\alpha) - \beta] \sin \alpha\,(t-x) d\alpha \tag{15a}$$

$$M(\alpha) = \sum_{j=1}^{4} \alpha m_j A_j \tag{15b}$$

$$\beta = \lim_{\alpha \to \infty} M(\alpha) = -\frac{\kappa + 1}{4} \tag{15c}$$

Since the contact area *a* and the contact stress $p(x)$ are unknowns in the singular integral Eq. (14), to complete the solution of the problem, contact stress $p(x)$ must satisfy the following equilibrium condition.

$$\int_{-a}^{a} p(t)\, dt = P \tag{16}$$

4. On the solution of the singular integral equation

This section is devoted to the numerical solution of the singular integral Eq. (14), Eqs. (15) by the Gauss-Chebyshev method. The singular integral and equilibrium condition of Eq. (16) will be converted to the dimensionless form by using the following normalized quantities.

$$s = x/a, \qquad t = r/a \tag{17a}$$

$$\varphi(r) = \frac{p(r)}{P/h} \tag{17b}$$

Using these normalized quantities, the integral in Eq. (14) and the equilibrium condition in Eq. (16) can be written as

$$\frac{1}{\pi}\int_{-1}^{1} \varphi(r)\left[\frac{1}{r-s} + \frac{a}{h}k(s,r)\right] dr = \frac{\beta}{R/h}\frac{\mu_0}{P/h}\frac{a}{h}s \tag{18}$$

$$\frac{a}{h}\int_{-1}^{1} \varphi(r)\, dr = 1 \tag{19}$$

Since there is smooth contact at the end points, the index of the integral Eq. (18) is – 1 [31]. The solution of the integral equation can thus be expressed as

$$\varphi(r) = g(r)\sqrt{(1-r^2)} \tag{20}$$

where $g(r)$ is a continuous and bounded function in the interval [–1, 1]. Applying the conventional collocation technique in [31, 32], the integral Eq. (18) can be transformed into the equivalent system of algebraic equations as follows

$$\sum_{i=1}^{N} W_i^N \left[\frac{1}{r_i - s_k} + \frac{a}{h}k(s_k, r_i)\right] g(r_i) = \frac{\beta}{R/h}\frac{\mu_0}{P/h}\frac{a}{h}s_k, \qquad k = 1,\ldots N+1 \tag{21}$$

and the equilibrium condition becomes

$$\frac{a}{h}\sum_{i=1}^{N} W_i^N\, g(r_i) = \frac{1}{\pi} \tag{22}$$

where r_i and s_k are the roots of the related Chebyshev polynomials and W_i^N is the weighting constant as

$$r_i = cos(\frac{i\pi}{N+1}), \qquad i = 1,\ldots N \tag{23a}$$

$$s_k = cos(\frac{\pi}{2}\frac{2k-1}{N+1}), \qquad k = 1,\ldots N+1 \tag{23b}$$

$$W_i^N = \frac{1-r_i^2}{N+1} \tag{23c}$$

Note that there are $N+1$ equations to determine the N unknowns $g(r_i)$ in Eq. (21). Since the extra equation is used to normalize the interval of integration, it is sufficient to choose only N of the $N+1$ possible collocation points (Krenk, 1975). Thus, Eq. (21) and Eq. (22) give $N+1$ equations to determine the $N+1$ unknowns, which are $g(r_i)$ and a. The system of equations is linear in terms of the $g(r_i)$ but highly nonlinear in variable a. Therefore, an iterative method is used to obtain the unknowns.

5. Numerical results

This section presents the effects of the foundation parameters, inhomogeneity parameter, indentation load, and punch radius on the contact stress distribution in the frictionless indentation of a functionally graded elastic layer by a rigid cylindrical punch. The punch radius, layer height, and Kolosov's constant are taken as $R = 100$ m, $h = 0.5$ m, and $\kappa = 2$ in the following analysis.

Fig. 2 shows the effect of lower spring stiffness. k_l on contact stresses. The softer lower spring stiffness allows the layer to deform more easily. Since the decrease in the lower spring stiffness modulus k_l allows the layer to undergo larger deformations, the punch is embedded more into the layer due to the external load; therefore, the contact lengths increase, and the values of the contact stresses decrease as the external load is spread over a larger area.

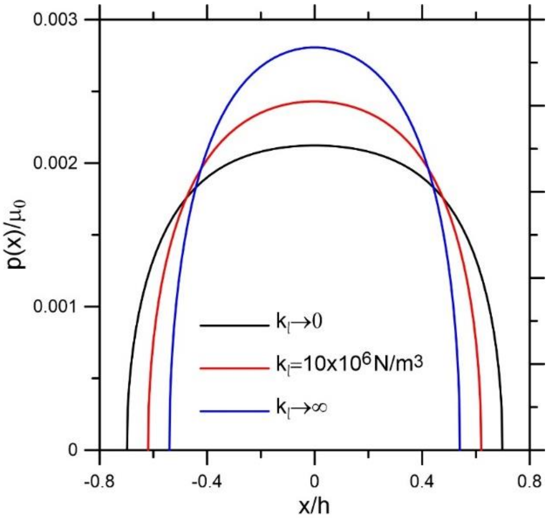

Fig. 2. The effect of the k_l on the contact stress ($P = 1 \times 10^7$ N/m, $\mu_h = 0.5\mu_0$, $k_s = 1$ GPa, $k_u = 100 \times 10^6$ N/m^3, $\mu_0 = 50$ GPa)

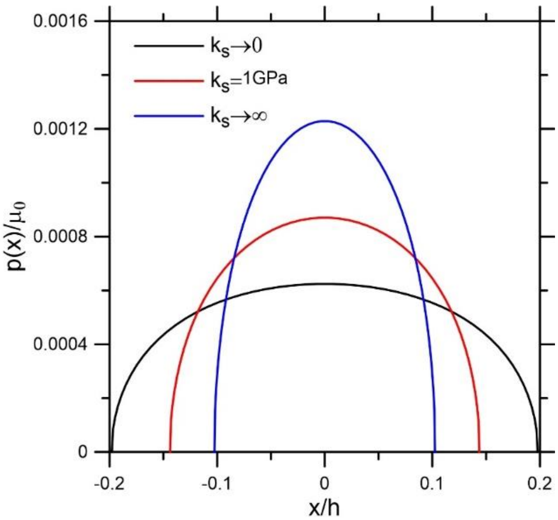

Fig. 3. The effect of the k_s on the contact stress ($P = 1 \times 10^7$ N/m, $\mu_h = 0.5\mu_0$, $k_s = 1$ GPa, $k_u = 100 \times 10^6$ N/m^3, $\mu_0 = 50$ GPa)

Fig. 3 shows the variation of contact stresses under the punch with the shear layer modulus, k_s. A softer shear layer increases the horizontal spread of contact stresses. This causes the contact stresses to spread over a wider area, while the maximum stress value decreases, creating a smoother, less abrupt stress distribution. Contact stresses reach their minimum values at $k_s = 0$. In the case of $k_s \to \infty$, the contact stresses spread over a more limited area and reach their maximum value on the axis of symmetry.

The upper spring modulus k_u represents the stiffness of the upper spring, which extends beneath the layer and directly interacts with it. The effect of the upper spring stiffness on the contact stress distribution under the punch is shown in Fig. 4. A decrease in the upper spring modulus allows the layer to deform more, thereby increasing the contact lengths under the punch while decreasing the peak contact stress. The maximum contact stress values are observed at $k_u \to \infty$.

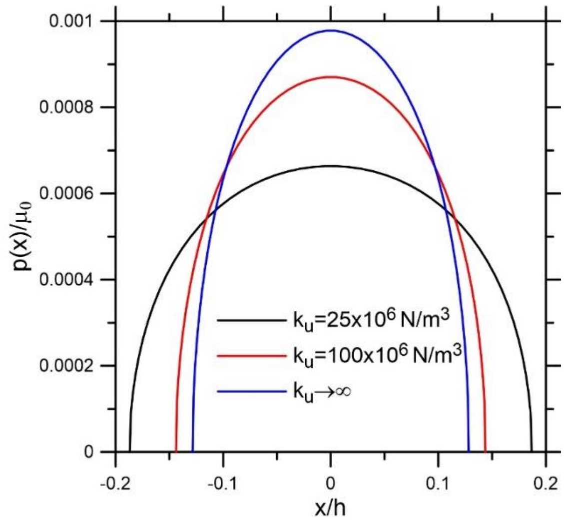

Fig. 4. The effect of the k_u on the contact stress ($P = 1 \times 10^7$ N/m, $\mu_h = 0.5\mu_0$, $k_s = 1$ GPa, $k_u = 100 \times 10^6$ N/m^3, $\mu_0 = 50$ GPa)

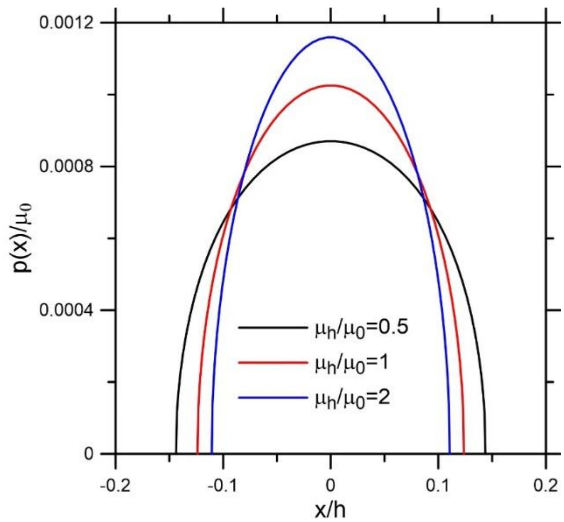

Fig. 5. The effect of the inhomogeneity μ^h/μ^0 on the contact stress ($P = 1 \times 10^7$ N/m, $\mu_h = 0.5\mu_0$, $k_s = 1$ GPa, $k_u = 100 \times 10^6$ N/m^3, $\mu_0 = 50$ GPa)

The effect of the inhomogeneity of the layer's stiffness on the distribution of contact stresses under the punch is shown in Fig. 5. The layer stiffness varies exponentially starting from the top surface of the layer. When $\mu^h/\mu^0 = 1$, the layer becomes homogeneous. As the layer's bottom stiffness increases relative to the top, the layer stiffness increases, while the contact lengths under the punch decrease.

The effect of the stiffness of the upper surface of the layer on the change in contact stresses under the punch is given in Fig. 6. With increasing values of μ_0, the total rigidity of the layer increases, and therefore, the rigid punch is less embedded in the layer due to the external load, and the peak value of the contact stresses increases.

Fig. 7 shows the effect of external load on the contact stress distribution under the punch. Unlike the effects of other parameters, both contact lengths and contact stresses increase with increasing external load. However, the shape of the contact stress distribution remains unchanged.

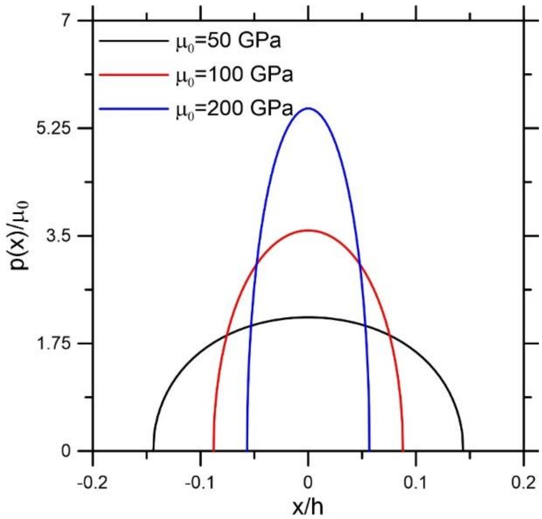

Fig. 6. The effect of the shear modulus μ_0 on the contact stress ($P = 1 \times 10^7$ N/m, $\mu_h = 0.5\mu_0$, $k_s = 1$ GPa, $k_u = 100 \times 10^6$ N/m^3)

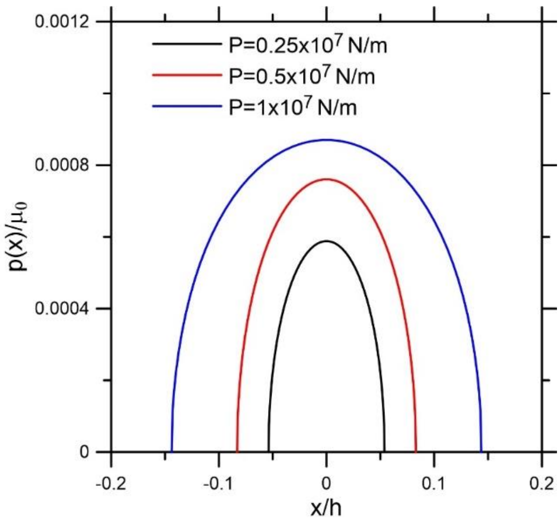

Fig. 7. The effect of the load P on the contact stress ($\mu_h = 0.5\mu_0$, $k_s = 1$ GPa, $k_u = 100 \times 10^6$ N/m^3, $\mu_0 = 50$ GPa)

6. Conclusion

The frictionless contact problem between a rigid cylindrical punch and an FG isotropic layer resting on a Kerr foundation is considered. The shear modulus of the layer is assumed to vary exponentially in the in-depth direction. The plane strain contact problem is solved using linear elasticity theory and the Fourier transform technique. From the numerical results, the following conclusions can be drawn:

- An increase in the Kerr foundation model parameters signifies an increase in the foundation stiffness, which results in a decrease in contact lengths. Consequently, the stress becomes concentrated in a narrow area, and the maximum value of the contact stress increases.
- A decrease in the Kerr foundation parameters leads to a softening, thereby causing the contact stress to spread over a wider area and exhibit a more uniform distribution. The rigid foundation condition (high parameter values) causes the stress distribution to "peak" within a narrow region.
- There is a positive correlation between the stiffness of the layer and the maximum contact stress; the changes in these parameters are in the same direction. A similar behavior has been observed for both the layer's surface shear modulus (μ_0) and the inhomogeneity parameter (μ_h/μ_0).
- When the applied external load P is increased, unlike the effect of other parameters, both the contact length and the maximum contact stress increase simultaneously.

CRediT authorship contribution statement

All authors contributed equally to this study. All authors have read and approved the final version of the manuscript and take equal responsibility for its content.

Declaration of conflicting interests

The author(s) declared no potential conflicts of interest with respect to the research, authorship, and/or publication of this article.

Funding

No funding was received for this study.

Data availability statement

The data that support the findings of this study are available from the corresponding author upon reasonable request.

References

[1] Long JM, Wang GF, Feng XQ, Yu SW (2012) Two-dimensional Hertzian contact problem with surface tension. Int J Solids Struct 49(13):1588–1594.
[2] Yusufoğlu E, Turhan I (2012) A mixed boundary value problem in orthotropic strip containing a crack. J Franklin Inst 349(9):2750–2769.
[3] Yusufoğlu E, Turhan İ (2013) A numerical approach for a crack problem by Gauss–Chebyshev quadrature. Arch Appl Mech 83(11):1535–1547.
[4] Çakıroğlu FL, Çakıroğlu M, Erdöl R (2001) Contact problems for two elastic layers resting on elastic half-plane. J Eng Mech 127(2):113–118.
[5] Yan J, Mi C (2017) On the receding contact between an inhomogeneously coated elastic layer and a homogeneous half-plane. Mech Mater 112:18–27.
[6] Alinia Y, Hosseini-Nasab M, Güler MA (2018) The sliding contact problem for an orthotropic coating bonded to an isotropic substrate. Eur J Mech A/Solids 70:156–171.

[7] Liu Z, Yan J, Mi C (2018) On the receding contact between a two-layer inhomogeneous laminate and a half-plane. Struct Eng Mech 66(3):329–341.

[8] Alinia Y, Espo M (2020) Sliding contact problem of an FGM coating/substrate system with two-dimensional material property grading. Acta Mech 231(2):649–659.

[9] Huang Z, Wen J (2025) A study of the receding contact problem for functionally graded piezoelectric materials. Math Mech Solids 30(8):1692–1710. https://doi.org/10.1177/10812865241296564

[10] Cao R, Mi C (2022) On the receding contact between a graded and a homogeneous layer due to a flat-ended indenter. Math Mech Solids 27(5):775–793.

[11] Çömez İ (2015) Contact problem for a functionally graded layer indented by a moving punch. Int J Mech Sci 100:339–344.

[12] Karabulut PM, Çetinkaya IT, Oğuz H, Çömez İ (2024) Moving contact problem of a functionally graded orthotropic coated half plane. Acta Mech 235(6):3989–4004.

[13] El-Borgi S, Abdelmoula R, Keer L (2006) A receding contact plane problem between a functionally graded layer and a homogeneous substrate. Int J Solids Struct 43(3–4):658–674.

[14] Öner E (2021) Computational contact mechanics for a medium consisting of functionally graded material coating and orthotropic substrate. J Struct Eng Appl Mech 4(4):249–266.

[15] Yan J, Li X (2015) Double receding contact plane problem between a functionally graded layer and an elastic layer. Eur J Mech A/Solids 53:143–150.

[16] Liu TJ, Yang F, Yu H, Aizikovich SM (2021) Axisymmetric adhesive contact problem for functionally graded materials coating based on the linear multi-layered model. Mech Based Des Struct Mach 49(1):41–58.

[17] Çömez İ, El-Borgi S, Kahya V, Erdöl R (2016) Receding contact problem for two-layer functionally graded media indented by a rigid punch. Acta Mech 227(9):2493–2504.

[18] Çömez İ (2022) Frictional moving contact problem between a functionally graded monoclinic layer and a rigid punch of an arbitrary profile. Acta Mech 233(4):1435–1453.

[19] Kahya V (2018) Plane receding contact problem for a functionally graded layer supported by two quarter-planes. Arch Mech 70(6):485–504.

[20] Ke LL, Wang YS (2007) Two-dimensional sliding frictional contact of functionally graded materials. Eur J Mech A/Solids 26(1):171–188.

[21] Kerr AD (1965) A study of a new foundation model. Acta Mech 1(2):135–147.

[22] Zhang L, Wu GT, Wu J (2019) A Kerr-type elastic foundation model for the buckling analysis of a beam bonded on an elastic layer. ZAMM J Appl Math Mech 99(10):e201900162.

[23] Tımeslı A (2022) Analytical modeling of buckling behavior of porous FGM cylindrical shell embedded within an elastic foundation. Gazi Univ J Sci 35(1):148–165.

[24] Shahsavari D, Shahsavari M, Li L, Karami B (2018) A novel quasi-3D hyperbolic theory for free vibration of FG plates with porosities resting on Winkler/Pasternak/Kerr foundation. Aerosp Sci Technol 72:134–149.

[25] Paliwal DN, Ghosh SK (2000) Stability of orthotropic plates on a Kerr foundation. AIAA J 38(10):1994–1997.

[26] Van Cauwelaert F, Stet M, Jasienski A (2002) The general solution for a slab subjected to centre and edge loads and resting on a Kerr foundation. Int J Pavement Eng 3(1):1–18.

[27] Do NT, Pham QH (2024) Nonlinear static analysis of functionally graded porous sandwich plates resting on Kerr foundation. Mech Adv Mater Struct 31(22):5678–5691.

[28] Zhang X, Zhao X, Li Y, Wang H, Zheng S (2025) Effect of flexoelectricity on the nonlinear thermo-electro-mechanical response of piezoelectric functionally graded porous graphene platelets-reinforced plates resting on the Kerr foundation. Acta Mech:1–33.

[29] Wu J, Ru CQ (2021) An analytical solution to the adhesive cylindrical indentation of a compressible elastic thin layer. J Adhesion 97(14):1291–1309.

[30] Alisjahbana SW, Alisjahabana I, Kiryu S, Gan BS (2018) Semi analytical solution of a rigid pavement under a moving load on a Kerr foundation model. J Vibroeng 20(5):2165–2174.

[31] Erdogan F, Gupta GDA, Cook TS (1973) Numerical solution of singular integral equations. In: Methods of Analysis and Solutions of Crack Problems. Springer, Dordrecht, pp. 368–425.

[32] Krenk S (1975) On quadrature formulas for singular integral equations of the first and the second kind. Q Appl Math 33(3):225–232.